

# Topography and Vegetation as Predictors of Snow Water Equivalent across the Alpine Treeline Ecotone at Lee Ridge, Glacier National Park, Montana, U.S.A.

Christine A. Geddes\*

Daniel G. Brown† and

Daniel B. Fagre‡

\*School of Natural Resources and Environment, University of Michigan, 430 E. University Avenue, Ann Arbor, Michigan 48109-1115, U.S.A.

Corresponding author present address: Institute for Fisheries Research, University of Michigan, 212 Museums Annex Bldg., Ann Arbor, Michigan 48109-1084, U.S.A. cgeddes@umich.edu

†School of Natural Resources and Environment, University of Michigan, 430 E. University Ave., Ann Arbor, Michigan 48109-1115, U.S.A.

danbrown@umich.edu

‡U.S. Geological Survey Northern Rocky Mountain Science Center, Glacier National Park, West Glacier, Montana 59936, U.S.A. dan\_fagre@usgs.gov

## Abstract

We derived and implemented two spatial models of May snow water equivalent (SWE) at Lee Ridge in Glacier National Park, Montana. We used the models to test the hypothesis that vegetation structure is a control on snow redistribution at the alpine treeline ecotone (ATE). The statistical models were derived using stepwise and “best” subsets regression techniques. The first model was derived from field measurements of SWE, topography, and vegetation taken at 27 sample points. The second model was derived using GIS-based measures of topography and vegetation. Both the field- ( $R^2 = 0.93$ ) and GIS-based models ( $R^2 = 0.69$ ) of May SWE included the following variables: site type (based on vegetation), elevation, maximum slope, and general slope aspect. Site type was identified as the most important predictor of SWE in both models, accounting for 74.0% and 29.5% of the variation, respectively. The GIS-based model was applied to create a predictive map of SWE across Lee Ridge, predicting little snow accumulation on the top of the ridge where vegetation is scarce. The GIS model failed in large depressions, including ephemeral stream channels. The models supported the hypothesis that upright vegetation has a positive effect on accumulation of SWE above and beyond the effects of topography. Vegetation, therefore, creates a positive feedback in which it modifies its environment and could affect the ability of additional vegetation to become established.

## Introduction

Snow is one of the more important influences on hydrologic, biologic, and climatic processes at the alpine treeline ecotone (ATE; Jones et al., 2001), which is defined as the gradient from tall, erect trees growing at normal forest densities to the harsher environmental conditions, biophysical disturbances, and competition at higher elevations that preclude tree survival. Snow is particularly influential on the distribution of plant communities at treeline, as it can offer plants protection from otherwise inhospitable conditions (Walker et al., 1993) as well as act as a stress and a disturbance (Walsh et al., 1994). Optimal depth of snow cover can protect plants against frost damage, dehydration, and wind abrasion (Wardle, 1968; Tranquillini, 1979). Snow also serves as a reservoir of water and essential nutrients (Bowman, 1992; Fisk et al., 1998). The timing of snowmelt is critical; deep snowpacks that persist into late spring or summer can shorten the growing season, while early snowmelt can lead to desiccation or the damping of phenological cycles (Billings and Bliss, 1959; Allen and Walsh, 1993). Thus, the presence of snowpatches can influence microenvironmental conditions, detrimentally or favorably, by reducing the growing season in some places and providing moisture in others where water might be limiting (Billings and Bliss, 1959; Rochefort and Peterson, 1996; Cairns and Malanson, 1998; Moir et al., 1999; Alftine et al., 2003).

Wind, topography, and vegetation interactions are important controls on snow accumulation and ablation, thereby influencing many ecological processes along the ATE (Walker et al., 1993). Vegetation itself plays an important role in treeline dynamics through positive-feedback switches with snow. Formally, a positive-feedback switch is defined as “a process in which a community modifies the environment, making it more suitable for that community” (Wilson and Agnew,

1992). Positive-feedback mechanisms are responsible for such distinctive vegetation patterns at the ATE as ribbon forest–snow glade alternating sequences (Billings, 1969) and isolated krummholz patches (Marr, 1977; Daly, 1984). In situations where snow serves to improve seedling establishment, snow can serve as one mechanism for positive feedback. For example, isolated patches of krummholz, surrounded by alpine tundra, form above treeline in depressions that are relatively protected from harsh conditions. Snow is scoured from tundra environments on ridge crests and subsequently transported downwind into krummholz patches and subalpine forest where trees act as snowfences, altering the local wind field and causing the formation of deep snowdrifts in the lee of the patch (Hiemstra et al., 2002). Melting occurs earliest in the growing season along the periphery of the snowpack, creating suitable moisture conditions and offering protection for seedling establishment without detrimentally shortening the growing season. Consequently, conditions to the lee of the patch can promote seedling establishment by improving the microclimate (Marr, 1977; Hättenschwiler and Smith, 1999). In this way, vegetation can act as an autogenic control on its environment.

This research contributes to a larger study that is attempting to explain the effects of positive-feedback strength, seed rain, and environmental gradients on the pattern of subalpine fir (*Abies lasiocarpa*), a common krummholz species in the northern Rocky Mountains. Malanson (1997) used simulation to identify at least two treeline patterns that can result from autogenic processes rather than abiotic spatial heterogeneity: a straight abrupt treeline and isolated patches. The relationships uncovered between snow and vegetation characteristics can help explain the mechanisms by which positive feedbacks affect vegetation pattern, and can be used to calibrate similar spatially explicit simulation models.

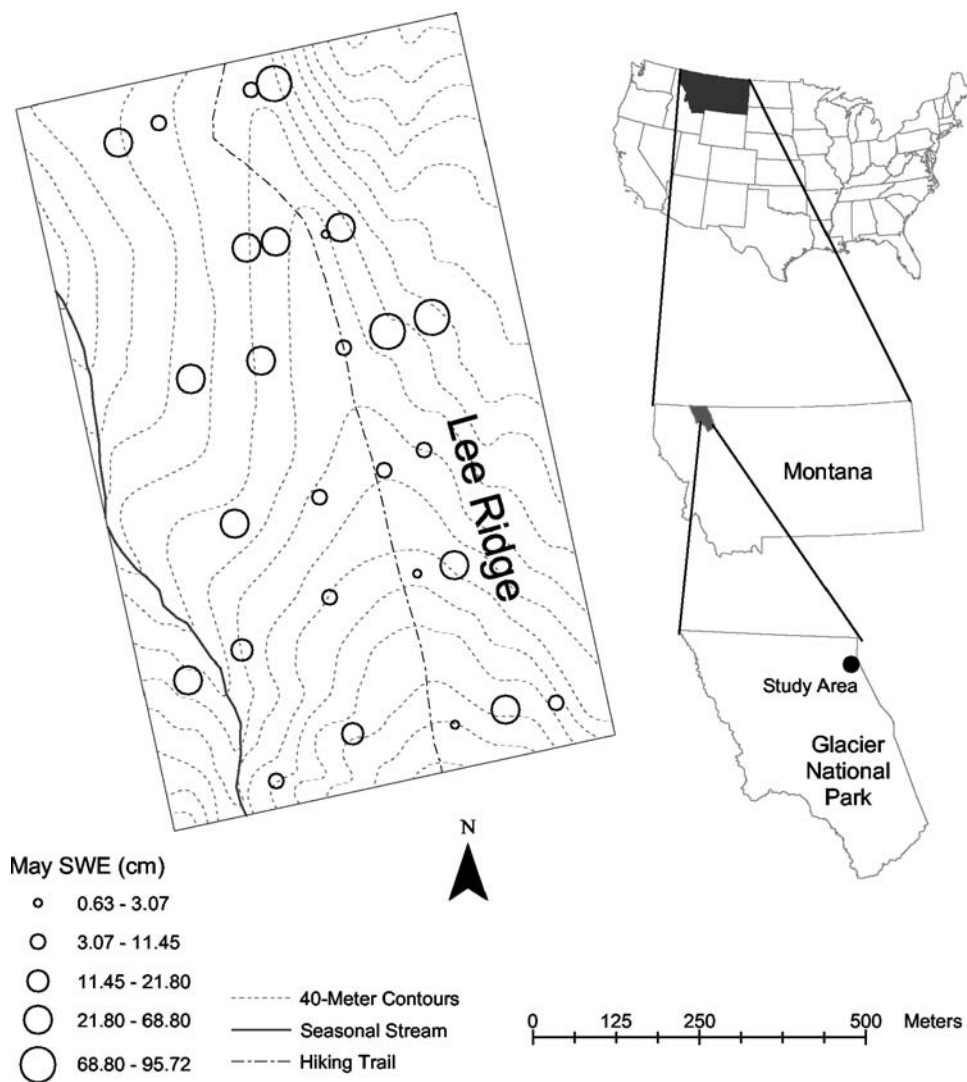


FIGURE 1. Location of study area in northeast Glacier National Park, Montana. Average May SWE, for 1999 through 2002, were based on measurements by field crews following the protocol of the Natural Resources Conservation Service (NRCS).

Predicting snow distribution in a geometrically complex landscape patterned with discontinuous vegetation structures is computationally and logistically difficult. Most studies to date have focused on modeling snow distribution over level terrain and are thus not applicable in mountain environments. A notable exception is the SnowTran-3D model developed by Liston and Sturm (1998), which has been applied at treeline in the Medicine Bow Mountains and the Northern Colorado Rocky Mountains (Greene et al., 1999; Hiemstra et al., 2002). The model simulates snow redistribution by wind over three-dimensional, complex terrain with variable vegetation cover. With inputs of solar radiation, precipitation, wind speed and direction, air temperature, humidity, topography, vegetation, and snow-holding capacity, the model calculates a wind-flow forcing field, wind-shear stress on the surface, transport by saltation and turbulent-suspension, loss to sublimation, and snow accumulation. The use of surrogate spatial variables for environmental processes may allow statistical modeling that can reduce the number of variables required without jeopardizing model integrity and, moreover, could facilitate remote collection (e.g., through remote sensing) of necessary data in rugged, often inaccessible, terrain.

The primary goal of this study was to test the hypothesis that, accounting for the effects of topography, vegetation structure is a significant control on snow redistribution at the ATE. The analysis was conducted by implementing spatial models of snow water equivalent (SWE) across the ATE on Lee Ridge in Glacier National Park, Montana, U.S.A. Snow water equivalent is the theoretical depth of

water if a snowpack were to instantaneously melt. It is preferred over snow depth as a measure of snow amount because of the spatial variability of snow density resulting from redistribution and differences in fresh snowfall (Goodison et al., 1981). A secondary methodological goal was to evaluate the possibility of using remotely sensed and geographic information system (GIS)-derived measures of these topographic and vegetation controls. Two statistical models were developed and compared: one using topographic and vegetation variables measured *in situ* and one using similar variables derived from remote sensing and processed variables using GIS. An advantage of the GIS-based model was the ability to apply it to data covering Lee Ridge to produce a predictive map of the distribution of SWE across the study site.

## Data and Methods

### STUDY AREA

The study area is in northeastern Glacier National Park in the northern Rocky Mountains of Montana, U.S.A. (Fig. 1). Glacier National Park lies astride the Continental Divide, and the Lee Ridge study site encompasses approximately 0.75 km<sup>2</sup> on its eastern flank. The Divide serves as a natural barrier separating two distinct climatic regimes; to the west of the Divide, a Pacific maritime climate dominates, and to the east of the Divide a drier continental climate prevails. Here the climate is characterized by long, severe winters and short, mild summers (Finklin, 1986).

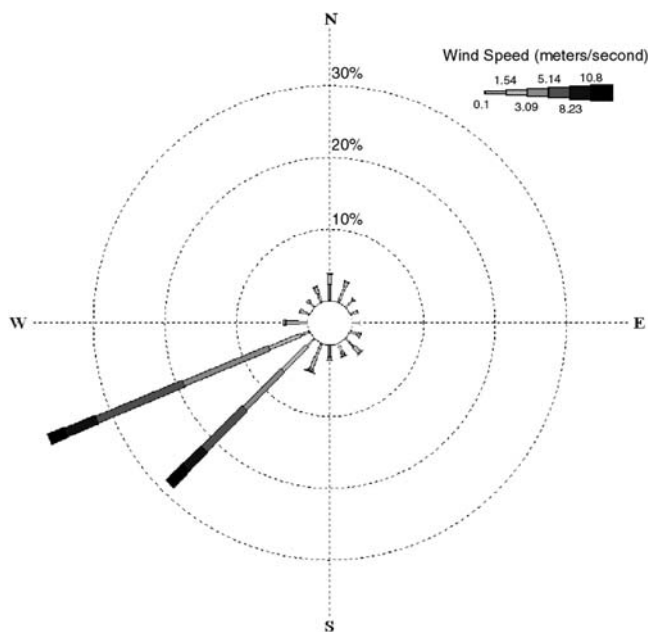


FIGURE 2. Wind rose. The wind direction frequencies are arranged in "petals" aligned with the wind directions, and the wind speed frequencies are shown using varying-width segments of the petals. Concentric circles represent the percentage of time wind of a given intensity comes from a given direction.

Previous studies have shown that topography is one of the most important factors regulating environmental processes in eastern Glacier National Park (Allen and Walsh, 1993, 1996; Brown, 1994a, 1994b; Walsh et al., 1994, 1998; Allen, 1998; Cairns, 1999, 2001). Elevations at the study site range from ca. 1985 m in the valleys on either side of the ridge to 2195 m at the top of the ridge. The terrain is rugged and rapid changes in elevation are common, especially on the eastern slope of the ridge and the areas beyond the valleys on either side of the ridge. Geomorphic disturbances, including rock and debris flows (Butler and Walsh, 1994), have left accumulations of talus at the base of many slopes. Evidence of fire (Kessel, 1979; Johnson and Larsen, 1991) and animal disturbances (Butler, 1992) also exists. Soil depths have not been shown to exhibit significant spatial variation across the ridge (Malanson et al., 2002).

Topographic interactions with wind are important in understanding snow, and consequently vegetation, distribution at the ATE. Data from a climatic station, continuously operating on Lee Ridge from 1998 through 2001 at a height of 10 ft (approx. 3 m) revealed a southwesterly prevailing winter wind direction with an azimuth of 225° from north (Fig. 2). These general wind patterns were in agreement with longer term records reported by Finklin (1986) for most areas in the Park.

Vegetation at the study site progresses from closed-canopy forest in the valleys to alpine meadows of fescue at mid-elevations to alpine tundra on the top of the ridge. Tree cover in the study area is dominated by subalpine fir (*Abies lasiocarpa*) and Engelmann spruce (*Picea engelmannii*) with some five-needle pines (*Pinus albicaulis* Engelm. and *P. flexilis* James). Lodgepole pine (*P. contorta*) is a dominant species over much of the western side of the ridge because of recovery from a historical fire event.

#### FIELD OBSERVATIONS

Snow depth and SWE data were collected by U.S. Geological Survey personnel along six snow courses, consisting of four to six sampling points each, extending from alpine tundra into subalpine

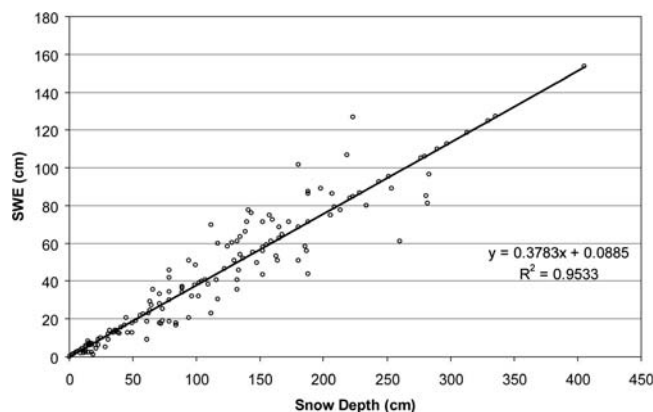


FIGURE 3. Snow Depth versus SWE. A total of 219 snow depth and SWE measurements, acquired between 1999 and 2002 on Lee Ridge, showed a strong positive relationship, so SWE was estimated for missing values based on this relationship where data were lacking.

forest on either side of the ridge (Fig. 1). The sites ranged in elevation from 2066 m to 2185 m. Snow data collection followed the protocol of the Natural Resources Conservation Service (NRCS; USDA, 1984). Though data were collected near the beginning of March, April, May, and June during each year from 1999 through 2002, we only used the May data. In addition to being the month with the most complete data set (i.e., fewest missing observations), May is also early enough to not have experienced a lot of melt yet late enough to have received most of the snow for the season. Measurements were recorded close to the beginning of the month; specific dates of visits were 3 May 1999, 8 May 2000, 25 April 2001, and 1 May 2002.

Variable field conditions resulted in substantial gaps in SWE measurements (ca. 20% of data values were missing from the data set). Snow depth plotted against SWE, based on measurements taken during all months of the 4-yr study period, yielded a strongly positive relationship ( $R^2 = 0.95$ ; Fig. 3). Snow water equivalent was therefore estimated for missing values based on this relationship. The measure of SWE we used was the average of the May SWE values across the four years (Fig. 1). Average May SWE values were, in general, greatest in forested areas on either side of the ridge and just beyond the eastern lip on the top of the ridge.

In addition to snow data, data were collected in the summer of 2002 to describe the topographic and vegetation conditions at each sample point (Table 1). Vegetation observations were made in four quadrants radiating 15 m from the respective snow posting. The length of the axes was believed to exceed any wind eddy influence from wind-forest canopy interaction (Greene et al., 1999). To capture the influence of strong winter winds, quadrants were oriented such that the axes were at a 45° angle to the prevailing winter wind direction. Quadrant axes were, therefore, oriented at 360° and 90°.

Vegetation structural characteristics thought to be relevant to snow redistribution were summarized in each quadrant. The relative proportions of trees, meadow, tundra/barren, and krummholz were noted at each site. In or near subalpine forest or krummholz patches, additional variables of interest included average vegetation height, distance to the nearest tree or treeline (as appropriate) in the SW direction, and the percent of each quadrant occupied by forest gaps. Artificially large values (i.e., 9999) were entered where distances to trees or treeline in the SW direction were so large as to prohibit measurement. Heights of representative samples of woody stems and distances were measured with a handheld digital laser rangefinder. Additionally, all sites were described using a structural site-type variable, defined in terms of proximity to tree cover in the SW direction as *forest*, *edge*, *edge/open*, or *open* (coded ordinally as "1", "2", "3",

TABLE 1  
Summary of all potential variables for the field-based model.

Variable	Explanation
Site type	Site type designation: <i>open</i> , <i>edge/open</i> , <i>edge</i> , or <i>forest</i> .
Distance to nearest tree in the SW direction	Distance (m) when appropriate.
Distance to treeline in the SW direction	Distance (m) when appropriate.
Proportion trees	Proportion tree cover ranging from 0 to 1, measured in NW, NE, SE, and SW quadrants.
Proportion meadow	Proportion meadow cover ranging from 0 to 1, measured in NW, NE, SE, and SW quadrants.
Proportion tundra/barren	Proportion tundra cover ranging from 0 to 1, measured in NW, NE, SE, and SW quadrants.
Proportion krummholz	Proportion krummholz cover ranging from 0 to 1, measured in NW, NE, SE, and SW quadrants.
Avg. tree height	Tree height (m) of a representative sample of trees, measured in NW, NE, SE, and SW quadrants.
Percent gaps	Percent gaps in the presence of tree cover, measured in NW, NE, SE, and SW quadrants.
Elevation	Elevation (m) at the location of the sampling site.
X coordinate	X coordinate in the UTM coordinate system acquired by a GPS receiver.
Y coordinate	Y coordinate in the UTM coordinate system acquired by a GPS receiver.
(X coordinate) <sup>2</sup>	Square of the X coordinate.
(Y coordinate) <sup>2</sup>	Square of the Y coordinate.
Aspect	Rescaled aspect ranging from -1 (NE) to +1 (SW).
Avg. max. slope	Average slope measured 3-m upslope and downslope in direction of maximum slope.
Profile curv.	Curvature over 6 m in the direction of maximum slope.
Avg. orthog. slope	Average slope measured both 3-m upslope and downslope from sampling point in direction orthogonal to maximum slope.
Plan curv.	Curvature over 3 m in the direction orthogonal to maximum slope.
Avg. SW slope	Average slope measured 3-m upslope and downslope in SW direction.
SW curv.	Curvature over 3 m in the SW direction.
General aspect	Aspect ranging from -1 to +1 indicating northeast-facing and southwest-facing slopes, respectively, measured along the continuous surface on which the sampling point was.
General slope	Slope measured along the continuous surface on which the sampling point was located.

and “4” in the model, respectively). Sites were designated *forest* if they were located within closed- or open-canopy forest, *edge* if they were proximal to treeline or a krummholz patch of large stature, *edge/open* if they were proximal to individual trees or a krummholz patch, and *open* if they were not proximal to upright vegetation.

Topographical measures of surface slope, aspect, and curvature were also recorded at each snow posting. Relative elevation measurements were made at locations 3 m from the sample points in each of four directions, oriented parallel and perpendicular to the maximum slope. An apparatus made of two posts, each having a protractor secured to it, and cord running between them was fashioned to make these measurements. These measurements were used to derive slope and profile and plan curvature, as well as slope and curvature in the SW direction. When the SW aspect (i.e., 210°) differed by less than 15° from either the direction maximum slope or its orthogonal, measurements made in these directions were used in place of separately making measurements in the SW direction. Curvature values range from -1 to +1, representing maximum concavity and maximum convexity, respectively. In addition, a measure of general slope and aspect was recorded. Slope and aspect were measured with a compass over the broad area, defined by breaks in terrain continuity (i.e., rapid changes in slope or aspect) around the sampling site. All measures of aspect were scaled to the range -1 to +1, representing northeast-facing and southwest-facing slopes, respectively.

#### GIS-BASED DATA

Alternative measures of terrain and vegetation structure were derived remotely and processed within a GIS. All GIS-based variables are summarized in Table 2.

#### Terrain Data

A digital elevation model (DEM) of the Lee Ridge area was generated using a series of 37 ground control points (GCPs) with elevations determined with differential GPS and a stereo pair of high-

resolution aerial photographs (scale: 1:15,000; Geddes, 2003). The automatic DEM extraction algorithm of OrthoEngine (PCI, Inc., Richmond Hill, Ontario) was used to extract elevation values and output them to a 5-m resolution DEM (Fig. 4A). The accuracy of the DEM was evaluated using two different data sets and compared against the 30 m DEM from the USGS (USGS, 1987). First, the DEM was compared with the GPS-based ground control points that were used to create the DEM. The calculated root mean squared error (RMSE) of the DEM was 9 m. Though this was a higher level of average error than the USGS DEM (6 m), both DEMs had errors (i.e., difference from the control points) that were less than 7 m for about two-thirds of the sample points. Further, the highest errors were observed in the valleys adjacent to the ridge, i.e., outside the area of interest. In a second evaluation, we compared the DEM with a total of 278 points collected within a small portion of the study area using a total station theodolite (Topcon GTS-226), which had an accuracy of about 15 cm. The linear regression relationship between elevations in the DEM was strong ( $R^2 = 0.75$ ) and substantially stronger than that obtained for the USGS DEM ( $R^2 = 0.19$ ). Together the error analyses suggest that the 5-m DEM suffered some areas of large error, especially in the valleys to the east and west of the ridge, perhaps because of the influence of trees on DEM heights, but was superior to the USGS DEM in representing local surface form on the ridge, which is the primary concern in understanding snow redistribution.

Elevation and geographic coordinates were extracted directly from the DEM. Grids of slope, aspect, profile curvature, and plan curvature were created in ArcGIS. As with the field-based measures, aspect was scaled to range from -1 to +1, representing northeast-facing and southwest-facing slopes, respectively.

Measures of the general aspect and slope of a site were derived from a triangulated irregular network (TIN) that was created from the DEM. Each triangle of a TIN represents a plane with a single slope and aspect over the contained area. The junctions of the planes, then, represent breaks in the terrain beyond a defined threshold. “Z tolerance” describes the degree of generalization applied in converting a gridded DEM to a TIN. Higher Z-tolerance values suggest more

TABLE 2

Summary of all potential remotely-acquired model variables. Data were extracted from a DEM, or its derivatives, of the study area or a vegetation classification in a GIS.

Variable	Explanation
Site type	Site type designation: <i>open, edge, or forest.</i>
Proportion trees/krum.	Proportion tree/krummholz cover ranging from 0 to 1, measured in NW, NE, SE, and SW quadrants.
Proportion meadow	Proportion meadow cover ranging from 0 to 1, measured in NW, NE, SE, and SW quadrants.
Proportion tundra	Proportion tundra cover ranging from 0 to 1, measured in NW, NE, SE, and SW quadrants.
Proportion snow	Proportion snow cover ranging from 0 to 1, measured in NW, NE, SE, and SW quadrants.
Elevation	Elevation (m) at the location of the sampling site.
X coordinate	X coordinate in the UTM coordinate system.
Y coordinate	Y coordinate in the UTM coordinate system.
(X coordinate) <sup>2</sup>	Square of the X coordinate.
(Y coordinate) <sup>2</sup>	Square of the Y coordinate.
Aspect	Aspect ranging from -1 (NE) to +1 (SW).
Avg. max. slope	Average slope measured in a 5-by-5-meter neighborhood (5-meter cell size) in direction of maximum slope.
Profile curv.	Curvature over 10 m in the direction of maximum slope.
General aspect	Aspect ranging from -1 (NE) to +1 (SW), measured on the TIN facet of the sampling point.
General slope	Slope measured on the TIN facet of the sampling point.

generalization. The benefit of using a TIN in this study was its ability to describe the surface at a resolution coarser than the DEM. The TIN created for this purpose was created with a Z tolerance of 2.06 m (i.e.,  $[Z_{max} - Z_{min}]/100$ ), which resulted in an average triangle size of 4038 m<sup>2</sup>. Slope and aspect were extracted from TIN faces with snow sampling sites. The TIN was then transformed to a raster (i.e., pixel) file to be compatible with the modeling format requirements. Orthogonal slope, slope in the SW direction, and curvature in the SW direction were not found from the GIS data.

#### Vegetation Structural Data

Vegetation structural classes were mapped by classifying a 1-m resolution Airborne Data Acquisition and Registration (ADAR) multispectral image, acquired for the study area on 28 July 1999. An object-oriented (OO) classification approach was employed to identify vegetation objects that were, on average, much larger than the resolution of the imagery (Geddes, 2003). Using eCognition software (Definiens AG, Munich, Germany), we segmented the image into spatially contiguous and spectrally homogenous spatial clusters. Next, a minimum of

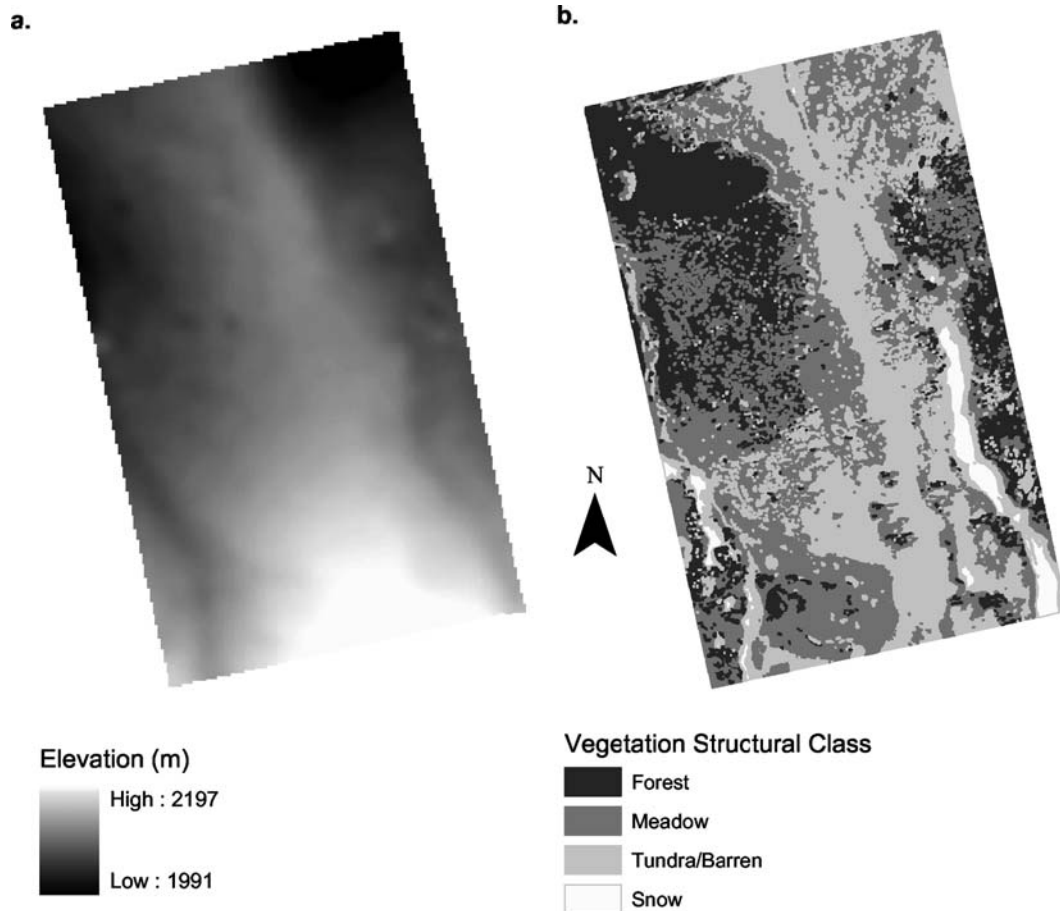


FIGURE 4. Digital data created for GIS-based model: (a) digital elevation model; (b) vegetation classification.

TABLE 3

Ordinary Least Squares models generated to explain May SWE across Lee Ridge. Two models were created: a field-based model using measures acquired in situ and a second model using only remotely acquired variables from a GIS. Measures of variable significance ( $t$ ), model fit ( $R^2$ ), and residual spatial autocorrelation (Moran's  $I$ ) are included for each model.

	May SWE (cm)	$t$ ( $P$ -value)	$R^2$	Moran's $I$
Field-based model	+466.20		0.93	-0.02 ( $P = 0.87$ )
	-18.63 (site type)	-11.62 (0.000)		
	-15.43 (gen. aspect)	-5.22 (0.000)		
	+0.98 (slope)	3.53 (0.002)		
	-0.19 (elevation)	-2.87 (0.009)		
GIS-based model	+736.60		0.69	-0.31 ( $P = 0.98$ )
	-21.92 (site type)	-3.96 (0.001)		
	-20.78 (gen. aspect)	-3.85 (0.001)		
	+1.41 (slope)	2.81 (0.010)		
	-0.32 (elevation)	-2.30 (0.031)		

20 of the resulting polygons was manually selected to represent each of four vegetation classes (i.e., forest, meadow, tundra/barren, and snow) as training polygons. A classification tree approach was used to develop rules to assign all polygons to one of these classes based on the spectral and spatial characteristics of the polygon (Fig. 4B). One hundred additional polygons were randomly selected and manually labeled for accuracy assessment in comparison with the classified map. Using a fuzzy accuracy assessment methodology (Gopal and Woodcock, 1994), we found that 95% of the evaluation polygons were assigned to the best class, determined by an image interpreter.

Proportions of vegetation classes within quadrants radiating 15 m from snow sampling sites were acquired in ArcGIS by summarizing land-cover types from the vegetation classification within wedges that mimicked field sampling dimensions and locations. Because of the vegetation classification scheme, there were two inconsistencies with field measurements; trees and krummholz were not distinguished in the classification and were, therefore, considered together, and snow was considered as a discrete class. *Forest*, *edge*, and *open* sites were identified by means of proxies from the vegetation classification. A 15-m radius wedge oriented to the SW ( $180^\circ$ – $270^\circ$ ) was superimposed on each site in the vegetation classification, and the cover type comprising the majority of the area was identified. Sites were then classified as forest, edge, or open (coded ordinally as “1”, “2”, and “4”, respectively) if the majority cover type in the SW direction was forest/krummholz, meadow, or tundra/snow, respectively. The *edgeloop* site type designation (coded “3” in the model generated by local measures) was omitted from the remote model derivation, as were distances to trees and treeline in the SW direction due to software limitations. Tree heights and percent forest gaps were difficult to ascertain without additional data and were, thus, not acquired digitally.

#### STATISTICAL MODELING

Statistical methods involved data exploration and the determination of a regression model that predicts average May SWE (in cm), followed by residual diagnostics. Two models were created and compared: one using the field-based measures as predictor variables and the other using GIS-based measures. The models were developed with a total of 27 observations. Though additional observations would improve the robustness of the findings, the intensive, multiyear effort required to collect the observations in a remote location limited our ability to increase the sample size without excessive cost.

The statistical models were fitted through an iterative process of model fitting in the Minitab statistical software package (Minitab, Inc., State College, PA). First, stepwise regression, recommended with large numbers of variables (Neter et al., 1996), was used to evaluate potential models with different numbers of variables. The stepwise regression formed the optimum combination of variables for explanation at each of progressive numbers of explanatory variables. Potential models were chosen based on model fit ( $R^2$ ). All variables suggested as potential predictors were then input for a best-subsets regression. The best-subsets algorithm searched for the best subsets from all variables in terms of predictability. Suitable models were then chosen based on their fit ( $R^2$ ), the numbers of variables in the respective models, and ecological defensibility. Because the process was highly iterative in nature, only the final models are presented below, with comments on interesting aspects of failed models. Variance inflation factors were calculated to evaluate the models for multicollinearity; values less than 10 are typically accepted to indicate a lack of multicollinearity effect on the model.

Satisfactory models were then implemented with an ordinary least squares (OLS) algorithm in ArcView GIS with the S-Plus extension (Mathsoft, Inc., Seattle WA). Residuals were investigated for violations of regression model assumptions. Linearity of relationships and normality and homoskedasticity of residuals were evaluated graphically using scatterplots, histograms, and plots of model predictions versus model residuals. The Moran coefficient (Bailey and Gatrell, 1995) was used to test for spatial dependence. Moran's  $I$  values vary from  $-1$  (i.e., negative spatial autocorrelation) to  $+1$  (i.e., positive spatial autocorrelation), with values significantly higher than zero suggesting that near values of residuals tend to be similar (i.e., not independent) and that Type I errors are possible. To generate a spatial weight matrix, which is necessary to compute the Moran coefficient, the point sampling locations were transformed into areas by generating Thiessen polygons. A matrix of first-order neighbor weights, which describes adjacent polygons as contiguous, was created and Moran's  $I$  calculated.

A map of “predicted” May SWE pattern was generated by applying the best regression model from the GIS-based variables to all raster cells on the ridge. This ability to map, i.e., “predict,” SWE at unmeasured locations is a distinct advantage of using GIS-based measures as predictors in the model.

## Results

Similar models were produced with field- and GIS-based predictor variables (Table 3). Stepwise and “best” subsets regression identified site type as the single best predictor of SWE in both models, accounting for 74.0 and 29.5% of the variation in May SWE, respectively. The best model in each case included site type, elevation, maximum slope, and general slope aspect. In addition, the field-based model included the proportion tree covered in the SE quadrant as a significant predictor, but that version of the model was rejected because of a high degree of collinearity between this variable and site type (variance inflation factor = 9.9).

The patterns of response of SWE to the predictor variables were similar between the models (Fig. 5). In each case, SWE decreased with increasing site type (which increased ordinally from forest sites through edge to open sites), elevation, and aspect relative to NE ( $-1$ ) and SW ( $+1$ ), and increased with increasing slope.

Analysis of error patterns revealed no significant violations of regression assumptions. Assumptions of residual normality and homoskedasticity were not violated, based on graphic analysis, nor were residuals spatially autocorrelated in either model (Table 3). The variance inflation factor values, as an indicator of multicollinearity in the model, were all less than 2.0.

The GIS-based model of average May SWE was applied to the entire study area, resulting in a 5-m resolution map of predicted SWE

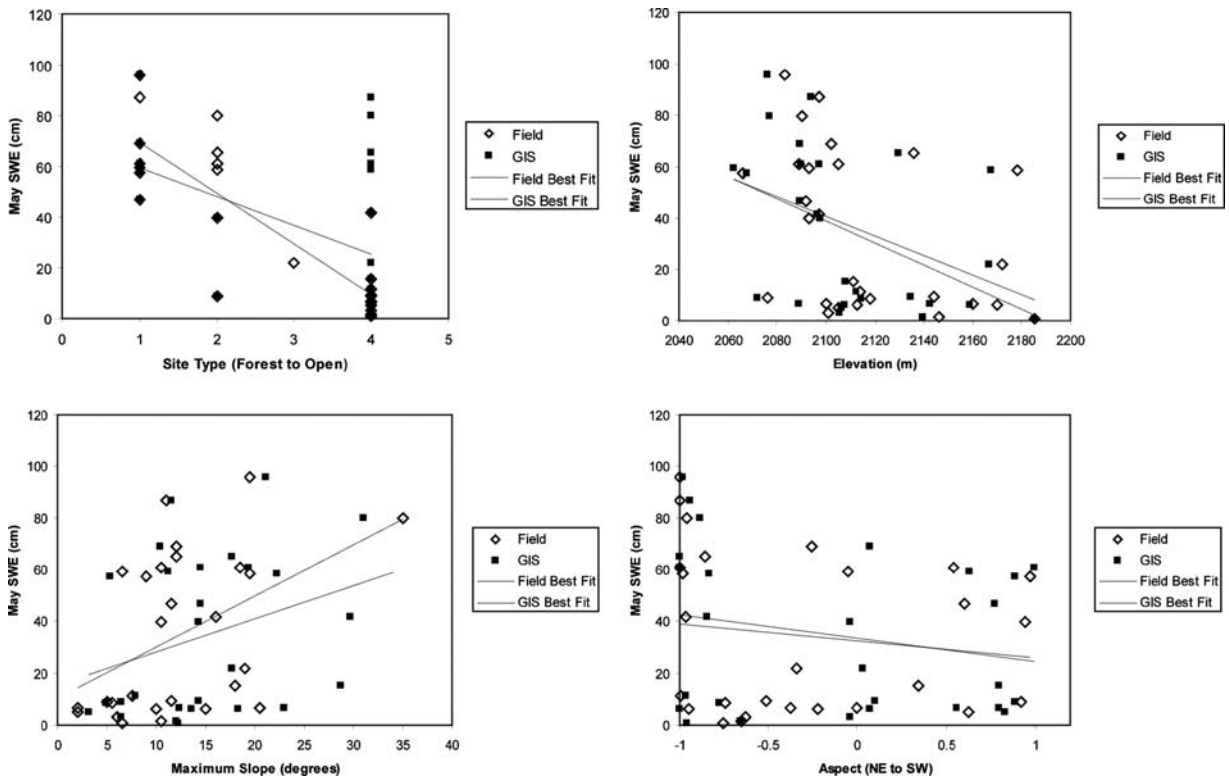


FIGURE 5. Predictor-response scatterplots of variables in the field- and GIS-based models.

(Fig. 6). Because of the small sample size no additional ground control data were available to evaluate the accuracy of the predictions. However, the fit of the model (Table 3) and the mapped output lend insight to model performance. The inclusion of general aspect data, which were derived from a TIN, propagated some of the sharp boundaries of the TIN faces. These were clearly discernible on an initial version of the predicted SWE map. For this reason, the version shown in Figure 6 was smoothed with a 5-by-5 averaging filter.

## Discussion

Together, vegetation and topography serve as important controls on snow distribution, resulting in distinct spatial patterning of snow accumulation at the ATE (Billings, 1969; Daly, 1984; Hiemstra et al., 2002). The statistical models developed here (Table 3) revealed a significant role of vegetation as a control on average May SWE, even while accounting for the topographic effects. In general, the highest SWE values were found to the lee of trees, where trees act as snow fences, promoting snowdrift accumulation. Snow water equivalent decreased in a sequence of site types from forest to forest edge, to edge/open, to open positions. On average, each step in the progression of site types, holding topographic variables constant, resulted in a reduction in SWE of 18.6 cm, based on the field-based model. The comparable value from the GIS-based model was 21.9 cm.

The models also demonstrated the importance of topography in controlling May SWE across Lee Ridge. In the field-based model, topographic measures alone accounted for 49.1% of the variation in SWE. Elevation, shown to be the most important determinant on treeline patterns (Brown, 1994a), is related to a complex of environmental gradients and, thus, is likely acting as a surrogate for other variables (e.g., wind speed and vegetation types). Also, sites oriented toward the NE (i.e., the leeward direction) accumulated more snow, most likely because of wind scouring on windward slopes, transport, and deposition. Interpretations of the effect of any individual variable in

the models must recognize variable interactions. For example, areas with the highest slopes on Lee Ridge are coincident with forest and meadow cover on the sides of the ridge, where vegetation serves as protection from harsh environmental conditions, and tundra/meadow communities just beyond the eastern lip on the top of the ridge, where snow accumulation can be explained by wind-topography relationships.

There are several potential sources of difference between the field- and GIS-based models. Different levels and types of data quality between the field and GIS-derived measures were clearly present. For example, differences in the resolution and accuracy of the topographic measures could have a large impact. Elevations in the DEM were likely over-estimated in areas of tall, dense vegetation. Even small changes in surface characteristics can have a large influence on wind speed, and thus on snow redistribution (Essery et al., 1999). Furthermore, some of the variables necessarily had slightly different definitions when derived in GIS compared to their field-based counterpart. For example, in the GIS-derived model site type was determined based on the vegetation map rather than observation and designation in the field.

Despite these potential differences, and despite a relatively small number of sample points, the two models were remarkably similar. Fit was strong in both models, though stronger in the field-based model ( $R^2 = 0.93$  vs.  $0.69$ ). The directions of relationships between SWE and the predictor variables were identical and the coefficients were similar. Thus, the forms of the models were very consistent. Though the GIS-based model was based strictly on remotely sensed information, we conclude that the information content, in terms of our ability to predict average May SWE, was similar to but not as good as information collected in the field at much greater expense.

The similarity of the field- and GIS-based models also suggests that the findings are robust despite the small sample size. If the findings were spurious because of small sample size, one might expect very different results given sets of predictor variables calculated by independent means. The consistency of relationships among the models suggests that the findings are not simply a result of “over-fitting” a small sample.

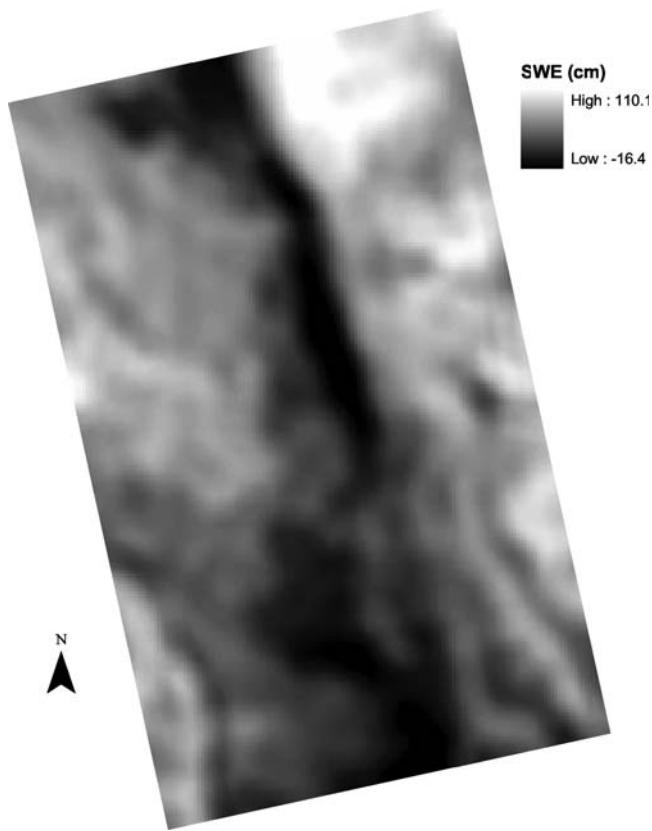


FIGURE 6. Predicted May SWE (cm) over Lee Ridge from a model calibrated with GIS-based measures of topography and vegetation.

Predicted patterns of SWE across the ridge, based on the GIS model (Fig. 6), were mostly consistent with expected results. SWE was predicted low on top of the ridge and higher at lower elevations on either side of the ridge where forest cover is dense. Two problematic areas were in the ephemeral stream channel to the west of the ridge and on the perennial snowfield in the valley to the east of the ridge. In both of these areas, where snow is known to accumulate in abundance, especially to the east, the model predicted relatively low SWE values. This resulted from the relative importance of site type in the model. The channels in the valleys are devoid of upright vegetation, while similar areas barren of tree cover tended to correspond to the upper, open areas on the ridge where wind scouring is great and SWE is low. Therefore, the model underestimated SWE in the valleys. This finding suggests that for prediction purposes, as with all statistical models, the model is limited to the relatively narrow range of conditions in which it was fitted.

### Conclusions

Two spatial models of SWE were derived for Lee Ridge in Glacier National Park, Montana as part of a larger study on treeline determinants: one calibrated with measures of topography and vegetation characteristics measured at 27 points *in situ* and one calibrated with similar measures acquired remotely and processed in a GIS. The GIS-based model was then applied to predict average May SWE across the study site. Both models included the variables site type (*forest*, *edge*, or *open*), elevation, maximum slope, and slope aspect, supporting the importance of topography (Brown, 1994a) and vegetation (Billings, 1969; Daly, 1984; Hiemstra et al., 2002) in determining snow redistribution across Lee Ridge.

The results provide evidence that the presence of upright

vegetation has a positive effect on accumulation of SWE while accounting for the effects of topography. As a result, the effect of snow can serve as a feedback in the formation of vegetation patterns at the ATE. The role of vegetation was made explicit in the models by the inclusion of site type. Notably, the site type variable relates to the wind protection from trees. SWE decreased from forest to forest edge to open positions, as trees act as snow fences and promote snowdrift accumulation (Marr, 1977; Hättenschwiler and Smith, 1999; Hiemstra et al., 2002). The GIS-based model had a lower fit ( $R^2 = 0.69$ ) than the field-based model ( $R^2 = 0.93$ ), possibly due to differences in data quality, variable definitions (i.e., site type), or scale issues. Despite these differences, the high degree of similarity of the models suggests that the findings are robust and that the small sample size did not lead to spurious model fits. The implementation of the GIS-based model across Lee Ridge predicted SWE to be lowest on the top of the ridge where wind scouring is the greatest and there is a paucity of upright vegetation. The model failed in areas of snowpatches and ephemeral stream channels, where snow is known to accumulate.

A logical next step in this research is to evaluate SWE model performance quantitatively. To do this, a substantially larger data set of field measurements is required to allow for model cross-validation. Additionally, new remote sensing technologies, like RADAR (Dobson et al., 1995) and LIDAR could be used to provide more direct estimates of the effects of three-dimensional vegetation structure on snow accumulation. Finally, the results of this research will contribute to a study of pattern and process relationships at the ATE and will be incorporated into a spatially explicit simulation model in which snow-vegetation feedbacks play a part in the formation of vegetation patterns.

### Acknowledgments

This is a contribution of the Mountain GeoDynamics Research Group. We gratefully acknowledge financial support for this work by the USGS Biological Resources Division (Cooperative Agreement No. 99CRAG0035) and the data collection efforts of our USGS colleagues Karen Holzer and Lisa McKeon.

### References Cited

- Alftine, K. J., Malanson, G. P., and Fagre, D. B., 2003: Feedback-driven response to multidecadal climatic variability at an alpine treeline. *Physical Geography*, 24: 520–535.
- Allen, T. R., 1998: Topographic context of glaciers and perennial snowfields, Glacier National Park, Montana. *Geomorphology*, 21: 207–216.
- Allen, T. R. and Walsh, S. J., 1993: Characterizing multitemporal alpine snowmelt patterns for ecological inferences. *Photogrammetric Engineering and Remote Sensing*, 59: 1521–1529.
- Allen, T. R. and Walsh, S. J., 1996: Spatial and compositional pattern of alpine treeline, Glacier National Park, Montana. *Photogrammetric Engineering and Remote Sensing*, 62: 1261–1268.
- Bailey, T. C. and Gatrell, A. C., 1995: *Interactive Spatial Data Analysis*. New York: J. Wiley, 413 pp.
- Billings, W. D., 1969: Vegetational patterns near alpine timberline as affected by fire-snowdrift interactions. *Vegetatio*, 19: 697–704.
- Billings, W. D. and Bliss, L. C., 1959: An alpine snowbank environment and its effects on vegetation, plant development, and productivity. *Ecology*, 40: 388–397.
- Bowman, W. D., 1992: Inputs and storage of nitrogen in winter snowpack in an alpine ecosystem. *Arctic and Alpine Research*, 24: 211–214.
- Brown, D. G., 1994a: Predicting vegetation types at treeline using topography and biophysical disturbance variables. *Journal of Vegetation Science*, 5: 641–656.
- Brown, D. G., 1994b: Comparison of vegetation-topography relationships at the alpine treeline ecotone. *Physical Geography*, 15: 125–145.



- Butler, D. R., 1992: The grizzly bear as an erosional agent in mountainous terrain. *Zeitschrift für Geomorphologie*, 36: 176–189.
- Butler, D. R. and Walsh, S. J., 1994: Site characteristics of debris flows and their relationship to alpine treeline. *Physical Geography*, 15: 181–199.
- Cairns, D. M., 1999: Multi-scale analysis of soil nutrients at alpine treeline in Glacier National Park, Montana. *Physical Geography*, 20: 256–271.
- Cairns, D. M., 2001: Patterns of winter desiccation in krummholz forms of *Abies lasiocarpa* at treeline sites in Glacier National Park, Montana. *Geografiska Annaler*, 83A: 157–168.
- Cairns, D. M. and Malanson, G. P., 1998: Environmental variables influencing the carbon balance at the alpine treeline: A modeling approach. *Journal of Vegetation Science*, 9: 679–692.
- Daly, C., 1984: Snow distribution patterns in the alpine krummholz zone. *Progress in Physical Geography*, 8: 157–175.
- Essery, R., Li, L., and Pomeroy, J., 1999: A distributed model of blowing snow over complex terrain. *Hydrological Processes*, 13: 2423–2438.
- Finklin, A. I., 1986: *A Climatic Handbook for Glacier National Park with Data for Waterton Lakes National Park*. U.S. Department of Agriculture, Forest Service, Intermountain Research Station, General Technical Report INT-204. 124 p.
- Fisk, M. C., Schmidt, S. K., and Seastedt, T. R., 1998. Topographic patterns of above- and belowground production and nitrogen cycling in Alpine tundra. *Ecology*, 79: 2253–2266.
- Geddes, C. A., 2003: Modeling Snow Water Equivalent at the Alpine Treeline Ecotone using Vegetation Structure and Topography Variables. Master's Thesis, University of Michigan, Ann Arbor. 111 pp.
- Goodison, B. E., Ferguson, H. L., and McKay, G. A., 1981: Measurement and data analysis. In Gray, D. and Male, D. H. (eds.), *Handbook of Snow, Principles, Processes, Management and Use*. Toronto: Pergamon Press, 191–274.
- Gopal, S. and Woodcock, C., 1994: Theory and methods for accuracy assessment of thematic maps using fuzzy sets. *Photogrammetric Engineering and Remote Sensing*, 60: 181–188.
- Greene, E. M., Liston, G. E., and Pielke, R. A., 1999: Simulation of above treeline snowdrift formation using a numerical snow-transport model. *Cold Regions Science and Technology*, 30: 135–144.
- Hättenschwiler, S. and Smith, W. K., 1999: Seedling occurrence in alpine treeline conifers: A case study from the central Rocky Mountains, USA. *Acta Oecologica*, 20: 219–224.
- Hiemstra, C. A., Liston, G. E., and Reiners, W. A., 2002: Snow redistribution by wind and interactions with vegetation at upper treeline in the Medicine Bow Mountains, Wyoming, U.S.A. *Arctic, Antarctic, and Alpine Research*, 34: 262–273.
- Johnson, E. A. and Larsen, C. P. S., 1991: Climatically induced change in fire frequency in the Southern Canadian Rockies. *Ecology*, 72: 194–201.
- Jones, H. G., Pomeroy, J. W., Walker, D. A., and Hoham, R. W. 2001: *Snow Ecology: An Interdisciplinary Examination of Snow-Covered Ecosystems*. New York: Cambridge University Press. 378 pp.
- Kessell, D. R., 1979: *Gradient Modeling: Resource and Fire Management*. New York: Springer-Verlag. 432 pp.
- Liston, G. E. and Sturm, M., 1998: A snow-transport model for complex terrain. *Journal of Glaciology*, 44: 498–516.
- Malanson, G. P., 1997: Effects of feedbacks and seed rain on ecotone patterns. *Landscape Ecology*, 12: 27–38.
- Malanson, G. P., Butler, D. R., Cairns, D. M., Welsh, T. E., and Resler, L. M., 2002: Variability in an edaphic indicator in alpine tundra. *Catena*, 49: 203–215.
- Marr, J. W., 1977: The development and movement of tree islands near the upper limit of tree growth in the southern Rocky Mountains. *Ecology*, 58: 1159–1164.
- Moir, W. H., Rochelle, S. G., and Schoettle, A. W., 1999: Microscale patterns of tree establishment near upper treeline, Snowy Range, Wyoming, U.S.A. *Arctic, Antarctic, and Alpine Research*, 31: 379–388.
- Neter, J., Kutner, M. H., Nachtsheim, C., and Wasserman, W., 1996: *Applied Linear Regression Models*, 3rd ed. Chicago: Irwin. 720 pp.
- Rochefort, R. M. and Peterson, D. L., 1996: Temporal and spatial distribution of trees in subalpine meadows of Mount Rainier National Park. *Arctic and Alpine Research*, 28: 52–59.
- Tranquillini, W., 1979: *Physiological Ecology of the Alpine Timberline: Tree Existence at High Altitudes with Special Reference to the European Alps*. New York: Springer-Verlag. 137 pp.
- U.S. Department of Agriculture (USDA), Natural Resources Conservation Service, 1984: *Snow Survey Sampling Guide*. Agriculture Handbook 169.
- U.S. Geological Survey (USGS), 1987: *Digital Elevation Models, Users Guide 5*. U.S. Geological Survey, Reston, Virginia.
- Walker, D. A., Halfpenny, J. C., Walker, M. D., and Wessman, C. A., 1993: Long-term studies of snow-vegetation interactions. *Bioscience*, 43: 287–301.
- Walsh, S. J., Butler, D. R., Allen, T. R., and Malanson, G. P., 1994: Influence of snow patterns and snow avalanches on the alpine treeline ecotone. *Journal of Vegetation Science*, 5: 657–672.
- Walsh, S. J., Butler, D. R., and Malanson, G. P., 1998: An overview of scale, pattern, process relationships in geomorphology: A remote sensing and GIS perspective. *Geomorphology*, 21: 183–205.
- Wardle, P., 1968: Engelmann spruce (*Picea engelmannii* Engel.) at its upper limits on the Front Range, Colorado. *Ecology*, 49: 483–495.
- Wilson, J. B., and Agnew, A. D. Q., 1992: Positive-feedback switches in plant communities. *Advances in Ecological Research*, 23: 263–336.

Ms submitted July 2003